Scanning Electron Microscopy

Volume 1986
Number 1 *Part I*

Article 9

4-14-1986

Physical Basis for Spectrometer Calibration

M. Gautier
Centre d'Etudes Nucleaires de Saclay

J. P. Duraud
Centre d'Etudes Nucleaires de Saclay

J. P. Vigouroux
Centre d'Etudes Nucleaires de Saclay

C. Le Gressus
Centre d'Etudes Nucleaires de Saclay

Follow this and additional works at: https://digitalcommons.usu.edu/electron

Part of the Biology Commons

Recommended Citation

Gautier, M.; Duraud, J. P.; Vigouroux, J. P.; and Le Gressus, C. (1986) "Physical Basis for Spectrometer Calibration," *Scanning Electron Microscopy*: Vol. 1986 : No. 1 , Article 9.
Available at: https://digitalcommons.usu.edu/electron/vol1986/iss1/9

This Article is brought to you for free and open access by the Western Dairy Center at DigitalCommons@USU. It has been accepted for inclusion in Scanning Electron Microscopy by an authorized administrator of DigitalCommons@USU. For more information, please contact digitalcommons@usu.edu.

SCANNING ELECTRON MICROSCOPY/1986/I (Pages 89-97)
SEM Inc., AMF O'Hare (Chicago), IL 60666-0507 USA

0586-5581/86$1.00+05

PHYSICAL BASIS FOR SPECTROMETER CALIBRATION

M. Gautier*, J.P. Duraud, J.P. Vigouroux, C. Le Gressus

IRDI - DESICP - DPC - SPCM - SES
Centre d'Etudes Nucléaires de Saclay
91191 GIF SUR YVETTE Cedex, FRANCE

(Received for publication April 03, 1985, and in revised form April 14, 1986)

Abstract

Progress in quantitative surface analysis is hampered by the lack of experimental procedure including spectrometer calibration, sample preparation, and general experimental setting-up. Two methods for spectrometer alignment are compared : the linearization method and the elastic peak test. Experimental spectra are presented, which can be considered as stringent reference data to check the instrument response and the analyser transmission at low energies.

Key Words: Spectrometer calibration, instrumental effect, quantitative Auger analysis.

*Address for correspondence:

M. Gautier
IRDI-DESICP-DPC-SPCM-SES
Centre d'Etudes Nucléaires de Saclay
91191 Gif sur Yvette Cedex
FRANCE
Phone n°: 69-08-50-77

Introduction

Chemical analysis of solid surfaces by electron spectroscopy is faced with several methodology problems, such as spectrometer calibration, and experimental procedure. As outlined by C.J. Powell (private communication), "there are now well over one thousand surface analysis instruments in the Member States of the VAMAS project (Versailles Project on Advanced Materials and Standards). There is, however, no agreed way of expressing a quantitative measurement of the surface composition and many other parameters".

Reference data are required in order to evaluate the correct setting up of the experiment. These reference data must be obtained from well defined standard samples, which can be prepared in a reproducible way. They have to be interpreted in connection with theoretically and experimentally known phenomena.

This paper deals with experimental results we obtained on pure monocrystalline aluminum samples < 111 > and < 100 > and polycrystalline copper; these data can be used as guidelines to check the spectrometer characteristics (alignment, transmission) and to define experimental procedures.

First, we compare two methods for spectrometer alignment, the linearization method defined by Peacock et al. (1984), and first and second derivative of elastic peak method, as we suggested in a previous paper (Le Gressus et al., 1983).

Then, results related with surface characterization, based on electron energy loss spectroscopy are presented. When the Al surface is atomically clean, its reconstruction can be followed on electron energy loss spectra and a 4 eV energy loss peak attributed to a transition between surface states is then observed at low accelerating voltage.

Finally, we verified that the analyser transmission in the low energy region (from 0 to 30 eV) does not produce any

spurious features. The secondary emission spectra of aluminum, similar to those obtained in other installations (Pillon et al. 1977), were compared with spectra deduced from Monte Carlo calculations (Ganachaud and Cailler, 1979).

Materials and Methods

Sample Preparation

Monocrystalline < 111 > and < 100> Aluminum, and polycrystalline copper samples were mechanically and electrochemically polished. They were rinsed in acetone before loading in the ultra-high vacuum chamber. Then they were cleaned in situ, by means of heating (500°C) and ion etching (Ar^+ ions, primary energy between 1 keV and 5 keV, beam intensity of a few μA per cm^2), until no contaminant was observed in Auger electron spectroscopy. Etching the sample gives a disordered surface ; we heated the sample afterwards to improve crystallinity.

Experimental Set-up

Experiments were carried out in a VG Escalab Mark II and JEOL Jamp 3.

The Mark II was pumped with liquid nitrogen trap diffusion pumps. The base pressure was between 5×10^{-11} and 5×10^{-10} mbar during the experiments. The system is fitted with an electrostatic electron gun (energy spread of around 1.5 eV), the energy of which can be easily varied between 100 eV and 10 keV. The Mark II is also equipped with an electron monochromator, the energy of which ranges from 0 eV to 100 eV (energy spread in this experiment of around a few tens of meV). The electrons are analyzed with a hemispherical mirror analyser (HMA) which can be operated either in constant analyser energy mode (CAE) (constant ΔE) or in constant retard ratio mode (CRR) (constant $\frac{\Delta E}{E}$). In the CAE mode, the distribution N(E) is obtained, whereas in the CRR mode, it is E.N(E).

In this experiment we used the CAE mode with a pass energy of 10 eV, which corresponds to an energy window ΔE = 1 eV.

The Jamp 3 was pumped with a titanium sublimation sputter ion pump. The base pressure was around 10^{-9} mbar. An electron optical system coupled with a bright and stable LaB_6 gun gives small electron probe of diameter 500 Å. The accelerating voltage can be varied between 100 eV and 30 keV. The Jamp 3 is equipped with a hemicylindrical mirror analyser (CMA), which permits one to record the E.N(E) distribution, with a constant resolution $\frac{\Delta E}{E}$ = 0.3%). Detection can be achieved in two modes: either synchronous detection with a lock-in amplifier, or the counting method. Geometry of Jamp 3 has been described by Le Gressus et al., 1983.

Alignment of the Spectrometer

In a recent paper, Peacock et al. (1984) proposed to adopt linearity in a plot of Log N (E) vs log E for energy values away from Auger lines to check the setting up of an experiment. We compared this criterion with the one we developed previously, which is based on the shape of the first and second derivatives of the elastic peak (Le Gressus et al. 1983).

Elastic peaks were recorded on Cu at 1225 eV in the Jamp 3 (CMA analyser), whereas linearization of the background was studied in the energy range 1 - 2 keV (energies greater than the LVV Auger peak) in the same apparatus with a primary energy beam of 15 keV.

When the spectrometer is completely misaligned as shown by the shape and the width of the elastic peak, the second derivative is very asymmetrical and log N(E) departs clearly from a straight line (figure 1). In the vicinity of the correct position (linearizable background and near symmetrical second derivative), the sensitivity of both methods was checked when the sample was submitted to small displacement (25 μm) along the z axis (figure 2). Both methods are sensitive to these variations. However it is impossible with the derivative to decide, owing to their similarity, which of the spectra is the correct one.

On the other hand, it is easier to see which background displays the wider linearizable part: on figure 2b for example, curve (2) shows a linear part over a wider range, from 1000 eV to 2000 eV, and then corresponds to the best alignment.

Therefore the linearization procedure appears as the most rigorous criterion to ascertain the correct setting up of the experiment.

Surface characterization

Studying the electron energy losses, in the reflection at a low energy (Ep ∿ 250 eV) provides a spectroscopy very sensitive to the surface: a weak contamination will produce modifications in the electron energy loss spectrum.

The electron energy losses on clean aluminum in the reflection mode have been extensively studied from the experimental point of view (Wendelken, 1976 ; Benndorf et al., 1977 ; Ichinokawa et al., 1981 ; Nall et al., 1981; Pellerin et al., 1981; Chiarello et al., 1984). The spectra were described according to the dielectric theory (Sevier, 1972 ; Powell and Swan, 1959), in correlation with aluminum optical data (Ehrenreich et al. 1963).

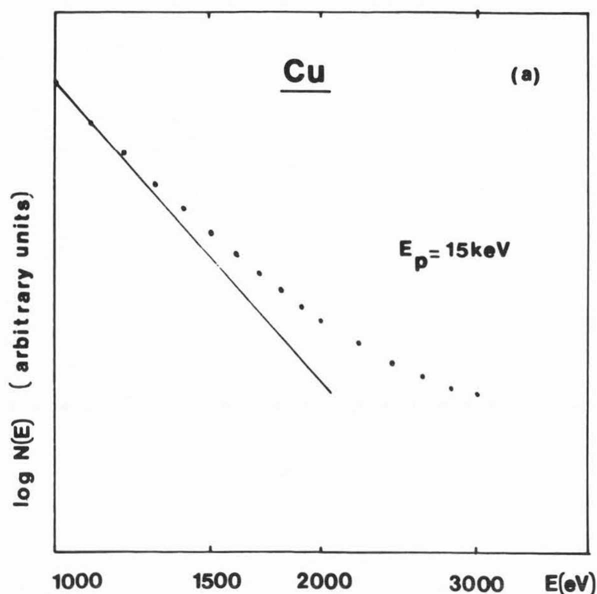

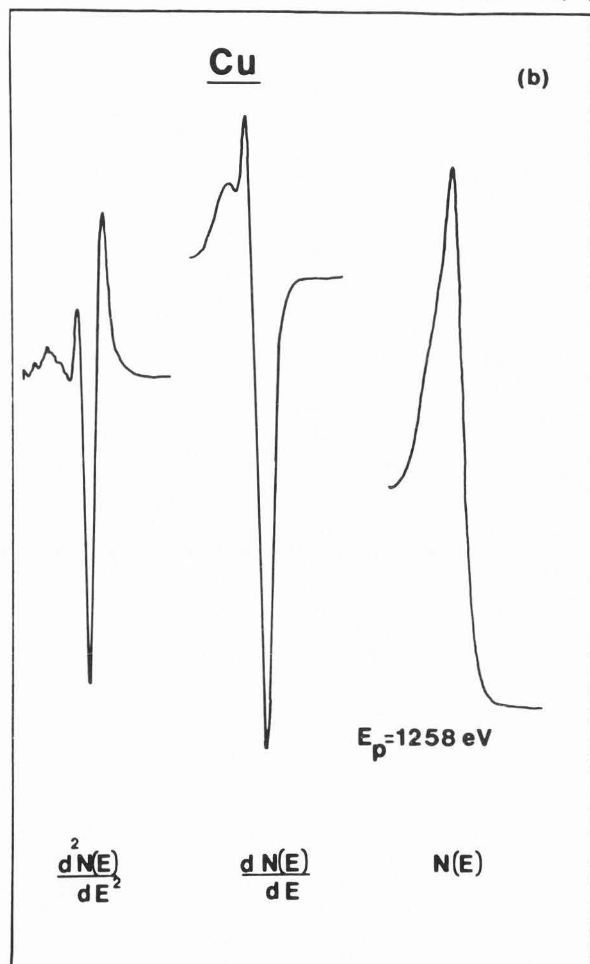

Fig. 1. Comparison between tests using either linearity (a) of the background or shape of the elastic peak (b), in the case of a misaligned spectrometer.

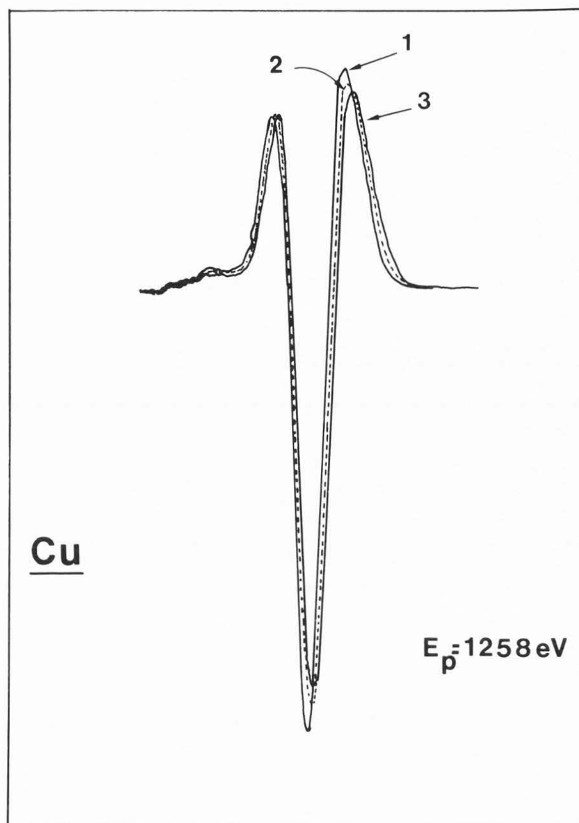

Fig. 2. Variation of the second derivative curve (a) and of the background in Log N(E) (b) with small displacement in the Z axis around the correct position. Curve 2: Z; curve 1: Z + 25 µm; curve 3: Z - 25 µm. The dashed vertical lines show the energy above which the experimental points depart by 20% from the linear plot.

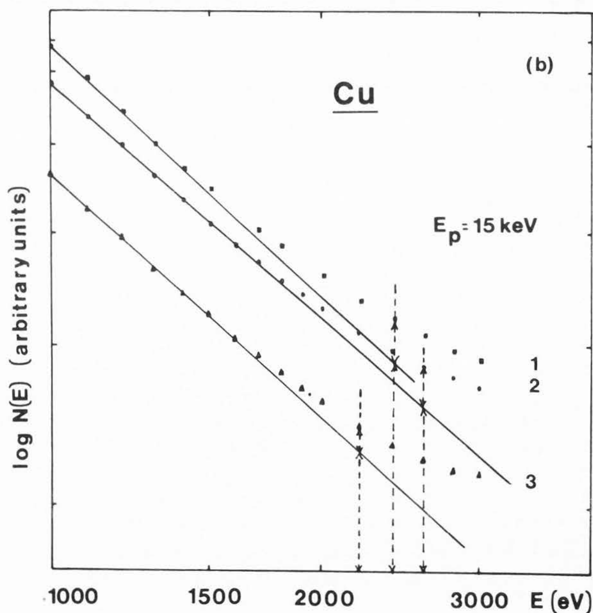

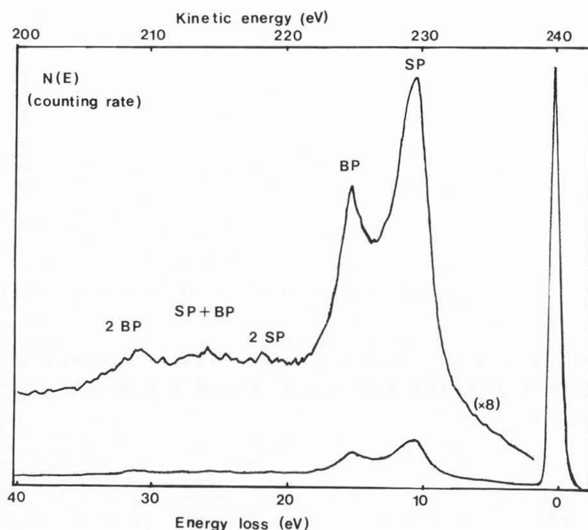

Fig. 3. Electron energy loss spectrum, on Al<111>, after ion etching. Ep=250 eV.

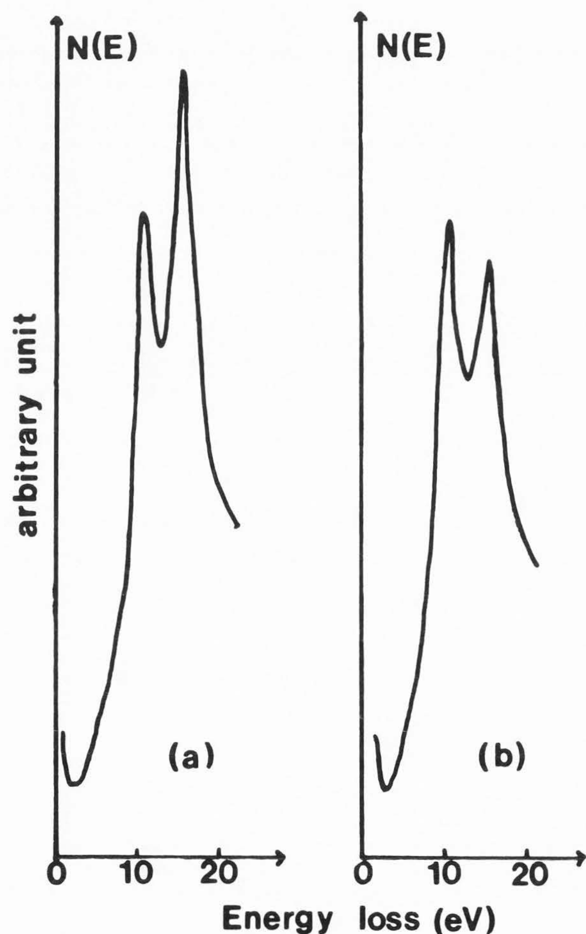

Fig. 4. Electron energy loss spectrum of clean Al<100> (Ep = 250 eV) - (a) after etching, disordered surface (b) after annealing, crystalline surface.

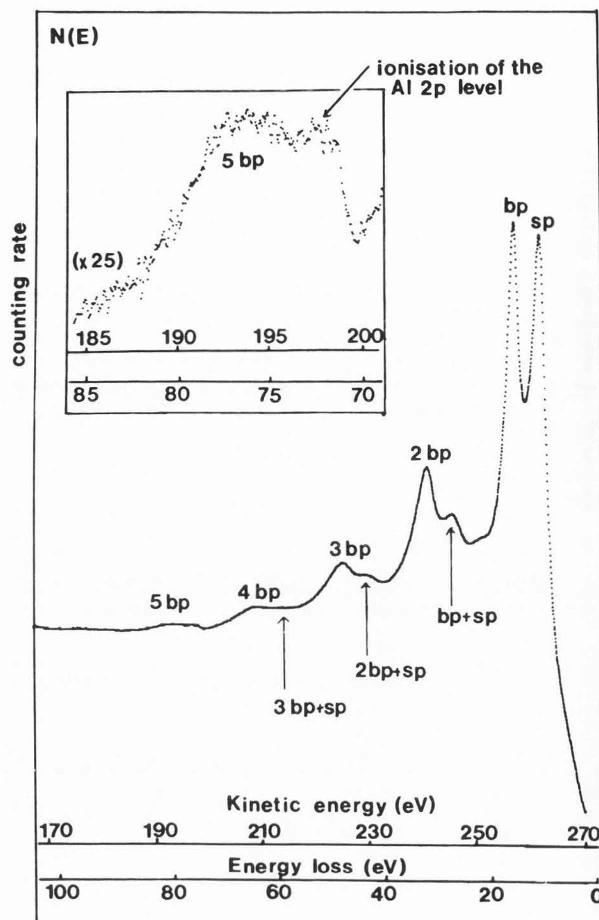

Fig. 5. Electron energy loss spectrum on clean Al<111>: multiple plasmon losses and excitation of the Al2p core level (Ep = 272 eV).

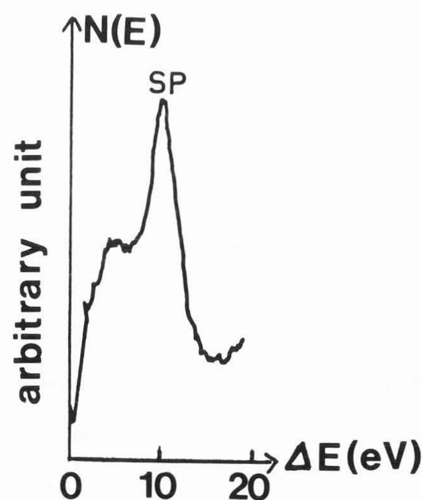

Fig. 6. Electron energy loss spectrum on clean Al<111>, with Ep = 50 eV.

A "quantitative approach" was realized by Stefani et al. (1984).

Figure 3 shows the electron energy loss spectrum obtained on clean Al <111>, just after etching. Features, which can be attributed to the excitation of a surface plasmon SP ($\Delta E = \hbar\omega_S = 10$ eV) and a bulk plasmon BP ($\Delta E = \hbar\omega_B = 15$ eV) can be seen, superimposed on the backscattered electron background. Structures attributed to the excitation of multiple plasmons (2 SP, SP + BP, 2 BP) as indicated on figure 3, can furthermore be observed. The energy loss corresponding to the excitation of two surface plasmons is very weak and is observed only when the surface plasmon peak is very intense. The ratio of the intensity of surface plasmon to bulk plasmon $\frac{SP}{BP}$ is characteristic of the surface cleanliness. The cleaner the surface, the more intense the ratio (Pellerin et al., 1981).

This ratio depends not only on the cleanliness of the surface, but also on the arrangement of the atoms on this surface: in fact, a spectrum recorded just after etching will be found modified if the surface is annealed after etching. Figure 4 represents the loss spectrum obtained on clean Al <100>, with a disordered surface (after ion etching), and with a crystalline surface (ion etching and annealing at 500°C). The ratio $\frac{SP}{BP}$ is then more intense on the crystalline surface than on the disordered one.

On a clean surface of aluminum, as depicted on figure 5 for Al <111>, multiple energy losses corresponding to the excitation of n BP + SP, n BP, can be seen for n = 1 to 6. As n increases, the intensity of the loss corresponding to n BP + SP decreases strongly. This result is in good agreement with that obtained by Van Attekum and Trooster, 1978.

A weak intensity peak is superimposed on the 5th bulk plasmon loss peak, at an energy $\Delta E \simeq 72.6$ eV (figure 5). This peak corresponds to the excitation of the 2p core level of pure aluminum.

When the accelerating voltage is decreased to Ep = 50 eV, a new peak, corresponding to an energy loss $\Delta E \sim 4$ eV can be observed. Figure 6 shows the energy loss spectrum obtained on clean and reconstructed Al <111>, with an electron monochromator. This peak was observed previously (Pellerin et al., 1981 ; Nall et al., 1981). As explained in a recent paper (Pellerin et al., 1984), the intensity of this peak, attributed to a transition between surface states, is strongly dependent on the primary energy and diffraction conditions. For increased accelerating voltage, for example Ep= 250 eV, the strong intensity of collective excitations (surface and bulk plasmons) can hide this transition peak, so that it is no longer seen distinctly on the N(E) curve.

Analyser Transmission at Low Energies

The low energy part of the electron emission curve corresponds to true secondary electrons.

The experimental secondary electron distribution of clean aluminum has been extensively studied (Guennou et al.,1974; Pillon et al., 1977 ; Everhart et al., 1976 ; Pellerin et al., 1981. Several models were proposed Henrich, 1973 ; Chung and Everhart, 1977 ; Ganachaud and Cailler, 1979) to explain the observed features superimposed on the cascade peak. These structures were correlated with the bulk and surface plasmon of aluminum.

Henrich's interpretation is based on the excitation of surface and bulk plasmon by secondary electrons leading to break points in the N(E) distribution, for energies around the plasmon energies.

Chung and Everhart propose that the surface and bulk plasmon decay gives rise to other secondary electrons, leading to small features superimposed on the cascade peak.

Figure 7 represents the secondary electron distribution obtained with the Mark II instrument, on clean Al <111>. Two broad features of weak intensity are observed around 10 eV and 15 eV, energies being referred to the Fermi level. These energies correspond to the plasmon energies $\hbar\omega_S$ and $\hbar\omega_B$.

This curve is in good agreement with the experimental curve of Pillon et al. (1977) and with the Monte Carlo calculation of Ganachaud and Cailler (1979), based on plasmon decay by creation of one or two electron-hole pairs (figure 8).

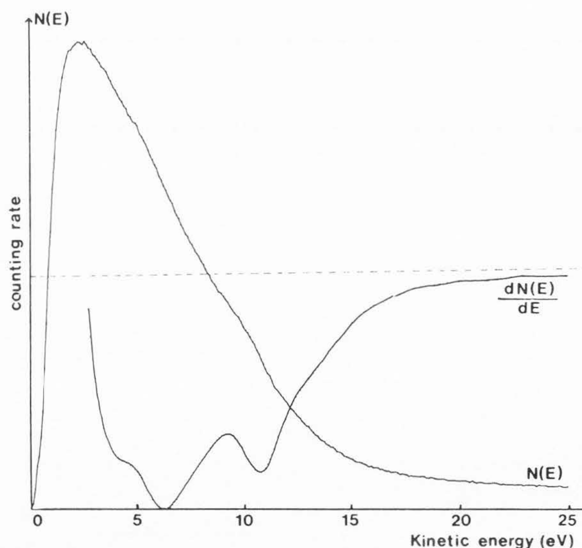

Fig. 7. Secondary electron spectrum on clean Al<111>, Ep = 250 eV. Energies are referenced to the vacuum level. To refer them to the Fermi level, one must add the analyser work function $\emptyset = 4.3$ eV.

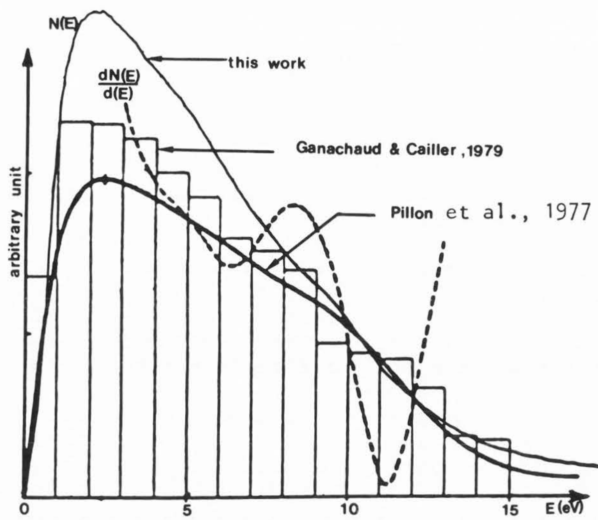

Fig. 8. Comparison between the experimental curve (Pillon et al., 1977), Monte Carlo calculation (Ganachaud and Cailler, 1979) and our experimental curve, on clean Al<111>.

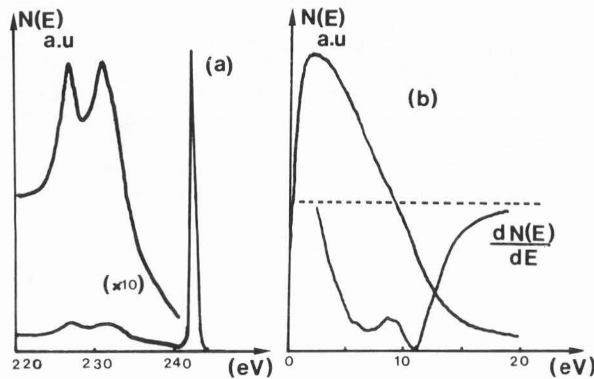

(c)

$\theta_i = 37°$

Fig. 9. Electron energy loss spectrum (a) and secondary electron spectrum (b) on clean Al<111>, (Ep = 243 eV); (c) geometry: Θ_i = 37°, Θ_f = 0°.

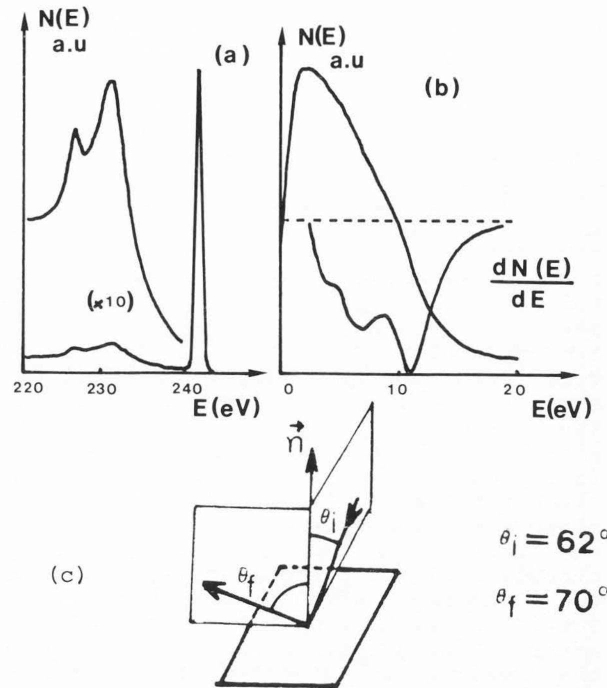

Fig. 10. Electron energy loss spectrum (a) and secondary electron spectrum (b) on clean Al<111> (Ep = 243 eV); (c) geometry: Θ_i = 62°, Θ_f = 70°.

In order to check the correlation existing between loss spectrum (bulk and surface plasmon excitation) and secondary electron distribution, we used two different geometries (figures 9c and 10c).

With the first one, the detection is in the direction normal to the sample (Θ_f = 0°) and the incidence angle Θ_i = 37°. With the second one, the incidence angle is Θ_i = 62° and the detection angle Θ_f = 70°. In the second case (grazing incidence and detection - fig. 10), the surface plasmon loss peak is more intense than in the first case (fig. 9), and the

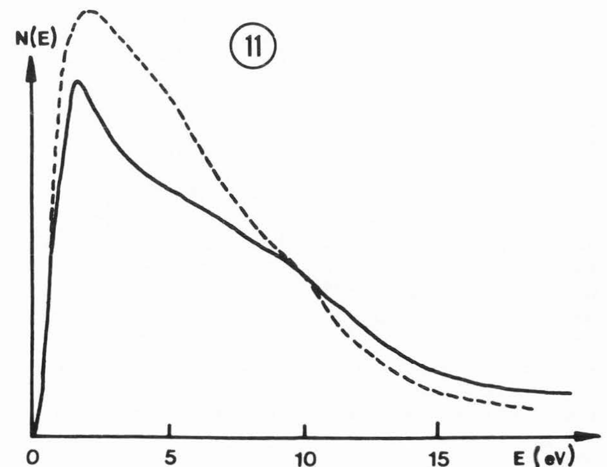

Fig. 11. Secondary electron spectrum (Ep = 250 eV) on clean Al<111>
_ _ _ correct distribution
______ in the presence of a weak stray magnetic field (B < 100 mG).

feature at 5 eV (referenced to the vacuum level) appears on the derivative of the secondary distribution more clearly (fig. 10b). This is in agreement with the interpretation of this feature as surface-plasmon decay leading to electron-hole pairs.

Furthermore, this part of the emission curve reflects the correct transmission of the spectrometer. In fact, when the analyser is misaligned or when weak stray magnetic fields are present in the chamber, the spectrum is distorted, and spurious features may appear (figure 11), even if no change is observed in the loss spectrum.

Conclusion

In order to propose guidelines for spectrometer calibration and experimental procedure, we compared two methods for spectrometer alignment. The linearization method is more sensitive to a weak misalignment than the elastic peak test (second derivative). Then we presented experimental spectra which can be considered as stringent reference data to check the instrumental response and the analyser transmission at low energies.

References

Benndorf C., Keller G., Seidel H., Thienne F. (1977). ELS Investigations of the beginning oxidation on aluminum thin films. Surf. Sci. 67, 589-595.

Chiarello G., Caputi L.S., Plutino S., Paolucci G., Colavita E., Decrescenzi M. , Papagno L. (1984). Aluminum collective excitations: reflection electron energy loss results. Surf. Sci. 146,241-255.

Chung M.S. , Everhart T.E. (1977). Role of plasmon decay in secondary electron emission in the nearly-free-electron metals. Application to aluminum. Phys. Rev. B 15 (10), 4699-4715.

Ehrenreich H, Philipp H.R., Segall B. (1963). Optical properties of aluminum. Phys. Rev. 132, 1918-1928.

Everhart T.E. , Saeki N. , Shimizu R., Koshikawa T. (1976). Measurement of structure in the energy distribution of slow secondary electrons from aluminum. Journal of Applied Physics, 47 (7), 2941-2945.

Ganachaud J.P. , Cailler M. (1979) A Monte Carlo calculation of the secondary electron emission of normal metals. Surf. Sci. 83, 498-518 (I - The model), 519-530 (II - Results for aluminum).

Guennou H. , Dufour G. , Bonnelle C. (1974). Emission électronique secondaire de cibles solides d'aluminium et de magnésium. Surf. Sci. 41, 547-554.

Henrich E. (1973). Role of bulk and surface plasmons in the emission of slow secondary electrons: polycrystalline aluminum. Phys. Rev. B, 7 (8), 3512-3519.

Ichinokawa T. , Le Gressus C. ; Mogami A. , Pellerin F. , Massignon D. (1981). Variation of relative intensities between surface and bulk plasmon losses due to crystal orientations for aluminum in low electron energy spectroscopy. Surf. Sci. 111, L 675-679.

Le Gressus C. , Geller J.P. , Le Moel A. (1983). Calibration-alignment-reproducibility using a cylindrical mirror analyser. Scanning Electron Microsc. 1983; II: 553-560.

Nall B.H. , Jette A.N. , Bargeron C.B. (1981). Electron Energy loss spectroscopy of <111> oriented aluminum single crystals. Surf. Sci. 110, L 606-610.

Peacock D.C., Prutton M., Roberts R. (1984). Instrumental effects in quantitative Auger electron spectroscopy. Vacuum 34 (5), 497-507.

Pellerin F. , Le Gressus C., Massignon D. (1981). A secondary electron spectroscopy and electron energy loss spectroscopy study of the interaction of oxygen with a polycrystalline aluminum surface. Surf. Sci. 103, 510-523.

Pellerin F., Langeron J.P. , Gautier M., Le Gressus C.(1984). Low energy electronic excitations of a clean Al(111) surface. Phys. Rev. B 30 (2), 1012-1015.

Pillon J, Ganachaud J.P., Roptin D. , Mignot H. , Dejardin-Horgues C. , Cailler M. (1977). Secondary electron emission of metal surfaces. Proc. 7th Intern. Vac. Cong. and 3rd Intern. Conf. Solid Surfaces, Vienne 77, ed. by R. Dobrozemsky et al., 473-476.

Powell C.J. , Swan J.B. (1959). Origin of the characteristic electron energy losses in aluminum. Phys. Rev. 115, 869-875.

Sevier K.D. (1972). Low energy electron spectroscopy. Wiley Interscience, New York, 278-284.

Stefani R. , Befeno B. , Allet R. (1984). A quantitative approach to electron energy loss spectroscopy on aluminum and silicon in the reflection mode. Scanning Electron Microsc. 1984; II: 601-606.

Van Attekum P.M. , Trooster J.M. (1978). Bulk - and surface - plasmon loss intensities in photoelectron, Auger, and electron energy loss spectra of Al metal. Phys. Rev. B 18 (8), 3872-3882.

Wendelken J.F. (1976). High-resolution temperature dependent inelastic low energy electron diffraction applied to the surface plasmon dispersion of aluminum (100). Phys. Rev. B 13 (12), 5230-5239.

Discussion with Reviewers

H.E. Bishop: In the practical alignment of the CMA, how do the two procedures compare for speed? Is it more efficient to use the elastic peak method to obtain an approximate alignment and then use the linearized cascade for the final adjustment or is it quicker to work simply with the cascade?
Authors: It is more efficient to use the elastic peak method to obtain a first alignment and then use the linearized cascade for the final adjustment: this procedure allows one to verify the alignment of analyser.
H.E. Bishop: How critical is the positioning of the specimen? You imply that in the JAMP 3 the specimen must be positioned within 25 μm. How precisely must the specimen be positioned in the Escalab II, and is this a function of the analyser mode?
Authors: As shown on figure 2b, we have checked that in JAMP 3, the linearization of background is sensitive to displacements of 25 μm along the Z axis, which correspond to 15 μm along the CMA axis, and 15 μm along the normal of the CMA axis.
In Escalab II, the positioning of specimen is not so critical as in JAMP 3. Peacock et al. (1984) have shown that the sample has to be positioned within 400 μm along the input lens axis, and within ± 200 μm of the centre of the CMA field of view to ensure an accuracy of better than ± 10% in estimates of Auger current. Preliminary results seem to indicate that there is no significant difference between the two analyser modes.
H.E. Bishop: Have crystalline effects, such as variations in the relative intensities of surface and bulk plasmons, proved to be a problem when using this approach to set up the spectrometer?
Authors: Owing to these crystalline effects we follow, for a given sample, the evolution of the ratio of bulk plasmon to surface plasmon with ion etching or sample heating, until a saturation value is reached.

C.J. Powell: Can you be more quantitative concerning the method recommended for spectrometer alignment? Over what electron energy range is the plot for copper in Fig. 2(b) linear? Have you made any measurements that correlate the extent of background nonlinearities (e.g. if the specimen is misaligned) with changes in relative Auger intensities as done by Peacock et al. (1984)?
Authors: As explained in the text, the plot 2 for copper in Fig. 2(b) is linear for a range 1000 eV-2000 eV. On Fig. 2(b) the dashed vertical lines represent the energy above which the experimental points depart by 20% from the linear plot. These energies are 2200 eV (curve 1); 2500 eV (curve 2); 2100 eV (curve 3).
In a previous paper (Le Gressus et al., 1983), it was shown that, in JAMP 3, translation of ± 100 μm along the CMA axis of symmetry caused variations in intensity of 50% for the SiKLL Auger line, and it was estimated that for an accuracy of ± 1% in intensity measurement, the sample would have to be reproducibly positioned to within ± 20 μm.

C.J. Powell: The proposed criterion for using the linearity of a plot of log N(E) versus log E for aligning the spectrometer and sample is useful in that it is a sensitive function of specimen-spectrometer distance. Nevertheless, this test which is based on the empirical observations of Sickafus [1977, Phys. Rev. B 16, (4), 1436-1447] and of Peacock et al. (1984) may not be "exact". Can the authors comment, either from the results of experiments with other materials or from other information, on the extent to which this alignment criterion is exact? For example, would two specimen materials of widely different atomic number be brought to alignment at the same position?
Authors: The description of the cascade in secondary electron emission by a power law: $B(E) = AE^{-m}$ has been justified by Sickafus both experimentally, in a study of spectra from clean metal surfaces, and theoretically by solution of the Boltzmann diffusion equation in the paper cited above. We have checked on samples with different atomic number C(Z=6), Si(Z=14), Cu(Z=29) and Au(Z=79) that alignment with the elastic peak test and with the linearization procedure lead to the same sample position, whatever the atomic number is.

M.P. Seah: In the measurements on polycrystalline copper did you notice any significant changes in the slope of the Log N(E) vs Log E plots on moving the electron beam from grain to grain?
Authors: In the experiments which are related in the paper, we did not study the variations of the m coefficient with the crystalline orientation. Such experiments are now in progress, in order to determine the influence of crystalline orientation of the m slope.

M.P. Seah: This point may or may not be important depending on the meaning the authors intended. The more intense surface plasmon may be observed by measuring the EELS either for grazing emission or, even more strongly, for grazing incidence and grazing detection angles. Now, the plasmon decays leading to peaks in the emitted spectrum would be proportional to

the excitation probability and so the surface plasmon peak would only be increased by use of the grazing incidence angles. Therefore, in the penultimate paragraph prior to the conclusions, the emphasis should be on the incidence and not the detection angle, even though they may be correlated in the instrument used here.

Authors: In the instrument described in the text, incidence and detection angle are correlated, as shown on fig. 9c and fig. 10c. Therefore when the incidence angle increases, the detection angle increases too, which explains the strong intensity of surface plasmon on fig. 10a, and the structure corresponding to surface plasmon decay clearly seen on the emission curve of fig. 10b.

M.P. Seah: One final point that appears to be confusing is that the surface plasmon emission peak in the secondary distribution spectrum occurs around 5 eV and the volume plasmon at 10 eV (these features would be the 10 and 15 eV seen in the EELS data if referred to the Fermi level). Yet in fig. 10 when the surface plasmon excitation is strongest in the EELS, we find that in the emission spectrum the opposite is the case and the volume plasmon at 10 eV is strongest.

Authors: Energies in the secondary emission spectra (figs. 7, 8, 9 and 10) are referenced to the analyser vacuum level. To refer them to the Fermi level, one must add the analyser work function ϕ = 4.3 eV. Therefore the structures observed in the emission spectrum have energies of $\sim$ 10 eV and $\sim$ 15 eV referred to the Fermi level, and correspond to surface and bulk plasmon decay by creation of electron-hole pairs (Chung and Everhart, 1977 ; Ganachaud and Cailler, 1979).

Surface (or bulk) plasmon decay, in the emission spectrum and surface (or bulk) plasmon excitation in the loss spectrum are correlated. Figs. 9 and 10 show that the more intense the surface plasmon excitation, the more intense the surface plasmon decay observed in the emission spectrum.

But we cannot simply compare the intensities of surface and bulk plasmon decay in the secondary emission spectrum because different production and escape depth are concerned.

M. Prutton: It is well known that N(E) falls with increasing energy at low energies and then rises towards the elastic peak at higher energies where backscattering becomes dominant. In a log-log plot the rise due to backscattered electrons will cause non-linearities at the high energy end. Do you attribute any of the curvature seen in the three plots of Fig. 2 to these backscattered electrons? If so can you separate such physical effects from the instrumental effects of specimen misalignment?

By working with primary energies of about 20 keV and analysing scattered electron energies below 2 keV, results using the CHA in the York SAM indicate that curvature in such log-log plots can be attributed entirely to instrumental effects. If the primary energy is reduced to 10 keV curvature due to backscattered electrons becomes observable above 1.5 keV.

Authors: On figure 12, we have plotted, for different primary energies E_p ranging from 3 keV to 20 keV the values E_c corresponding to the break point between secondary and backscattered electron distributions for a copper sample. For E_p = 10 keV for example, the curvature occurs for E_c = 1550 eV, which is in agreement with the value given by M. Prutton.

Therefore we estimate the curvatures seen in the three plots of figure 2b are due to the backscattered electrons.

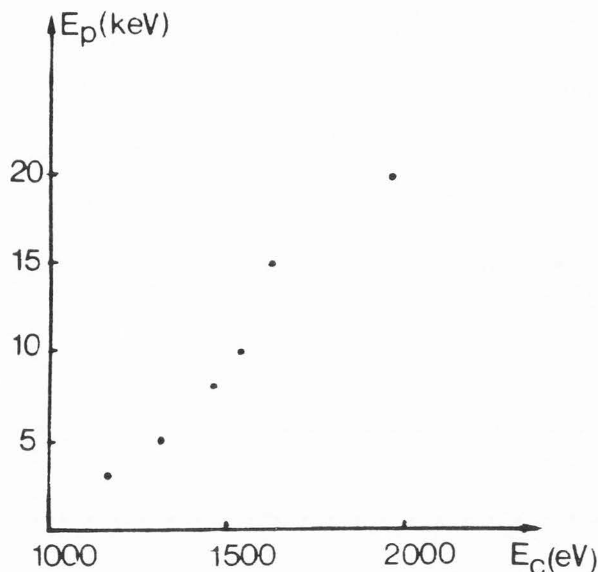

Fig. 12. Energy E_c corresponding to the break point between secondary and backscattered electron distributions, as a function of primary energy, for a copper sample.

Nevertheless, it is difficult to know accurately the backscattered electron intensities in this domain; this would require Monte Carlo calculation of the whole N(E) distribution. Such data exist [Shimizu R. and Ichimura S.(1981) . Quantitative Analysis by Auger Electron Spectroscopy. Monte Carlo calculations of electron backscattering effects. Toyota Foundation Research, Report. Rep. N°I-006], but with a poor statistics in this critical region, which makes difficult a precise interpretation of the curve into instrumental effect and physical effect.